Autonomic Neuroscience: Basic and Clinical 145 (2009) 55–62

Contents lists available at ScienceDirect

Autonomic Neuroscience: Basic and Clinical

journal homepage: www.elsevier.com/locate/autneu

Spatially divergent cardiac responses to nicotinic stimulation of ganglionated plexus neurons in the canine heart

René Cardinal [a,b,*], Pierre Pagé [a,c], Michel Vermeulen [a], Jeffrey L. Ardell [d], J. Andrew Armour [a,b]

[a] Centre de Recherche, Hôpital du Sacré-Cœur de Montréal, Canada
[b] Department of Pharmacology, Université de Montréal, Montréal, Québec, Canada
[c] Department of Surgery, Université de Montréal, Montréal, Québec, Canada
[d] Department of Pharmacology, East Tennessee State University, Tenn, United States

ARTICLE INFO

Article history:
Received 30 July 2008
Received in revised form 10 October 2008
Accepted 9 November 2008

Keywords:
Intrinsic cardiac nervous system
Cardiac mapping
Cardiac innervation
Heart rate
Nicotine cardiac ganglionated plexus

ABSTRACT

Ganglionated plexuses (GPs) are major constituents of the intrinsic cardiac nervous system, the final common integrator of regional cardiac control. We hypothesized that nicotinic stimulation of individual GPs exerts divergent regional influences, affecting atrial as well as ventricular functions. In 22 anesthetized canines, unipolar electrograms were recorded from 127 atrial and 127 ventricular epicardial loci during nicotine injection (100 mcg in 0.1 ml) into either the 1) right atrial (RA), 2) dorsal atrial, 3) left atrial, 4) inferior vena cava-inferior left atrial, 5) right ventricular, 6) ventral septal ventricular or 7) cranial medial ventricular (CMV) GP. In addition to sinus and AV nodal function, neural effects on atrial and ventricular repolarization were identified as changes in the area subtended by unipolar recordings under basal conditions and at maximum neurally-induced effects. Animals were studied with intact AV node or following ablation to achieve ventricular rate control. Atrial rate was affected in response to stimulation of all 7 GPs with an incidence of 50–95% of the animals among the different GPs. AV conduction was affected following stimulation of 6/7 GP with an incidence of 22–75% among GPs. Atrial and ventricular repolarization properties were affected by atrial as well as ventricular GP stimulation. Distinct regional patterns of repolarization changes were identified in response to stimulation of individual GPs. RAGP predominantly affected the RA and posterior right ventricular walls whereas CMVGP elicited biatrial and biventricular repolarization changes. Spatially divergent and overlapping cardiac regions are affected in response to nicotinic stimulation of neurons in individual GPs.

1. Introduction

The intrinsic cardiac nervous system is the final common regulator of regional cardiac function, processing parasympathetic and sympathetic efferent as well as cardiac sensory neuronal inputs (Armour, 2004). The intrinsic cardiac ganglia nested within epicardial fat pads are distributed with the greatest density at several intrapericardial loci identified in the canine heart (Lazzara et al., 1973; Yuan et al., 1994; Chiou et al., 1997; Pauza et al., 1999), a model which bears good correspondence to the human (Armour et al., 1997; Pauza et al., 2000). We have proposed a clinically relevant nomenclature (Yuan et al., 1994) given that the ganglionated plexuses are currently considered as potential targets for ablative therapy of cardiac arrhythmias (Pokushalov, 2008). Four are anatomically associated with atrial tissues: 1) the right atrial, 2) the inferior vena cava-inferior left atrial, 3) the dorsal atrial and 4) the left atrial ganglionated plexus, and three are associated with ventricular tissues: 5) the right ventricular, 6) the cranial medial ventricular ganglionated plexus and 7) its ventral septal ventricular component.

Histological descriptions of cholinergic nerve inputs to specific cardiac regions have been reported (Bojsen-Moller and Tranum-Jensen, 1971; Pauza et al., 2002). There is also a need for precise atrial and ventricular delineation of the functional responses to ganglionated plexus stimulation. Much attention has been devoted to the right atrial ganglionated plexus nested within fatty tissues at the right pulmonary vein-right atrial junction and to the one located at the inferior vena cava-inferior left atrial junction, each mediating relatively selective sinus and AV nodal regulation, respectively (Lazzara et al., 1973; Ardell and Randall, 1986; Gatti et al., 1995; Chiou et al., 1997; Tsuboi et al., 2000). The possibility exists that neuronal somata in individual ganglionated plexuses might exert spatially divergent effects, particularly that atrial neurons influence the ventricles (Takahashi et al., 1985; Blomquist et al., 1987).

Acetylcholine is the principal excitatory neurotransmitter in the intracardiac ganglionic synapse (Priola et al., 1977) and the evoked responses are mediated via nicotinic receptors (Smith, 1999). Small quantities of nicotine administered via the local coronary arterial

* Corresponding author. Centre de Recherche, Hôpital du Sacré-Cœur de Montréal, 5400 Gouin Boulevard West, Montréal, Québec, Canada H4J 1C5. Tel.: +1 514 338 2222x3180; fax: +1 514 338 2694.
E-mail address: rene.cardinal@umontreal.ca (R. Cardinal).

1566-0702/$ – see front matter © 2008 Elsevier B.V. All rights reserved.
doi:10.1016/j.autneu.2008.11.007

blood supply (Priola et al., 1977; Blomquist et al., 1987) or directly into the fatty tissues hosting the ganglionated plexuses cause modulation of intrinsic cardiac nerve activity and cardiac responses (Huang et al., 1993; Yuan et al., 1993) without tachyphylaxis (Blomquist and Priola, 1992). Locally administered nicotine selectively activates the somata and dendrites of adjacent intrinsic cardiac neurons without affecting axons of passage (Butler et al., 1990a,b). In contrast, electrical stimuli (Butler et al., 1990a, Quan et al., 1999, 2002; Tsuboi et al., 2000) may induce extensive cardiac effects via the concomitant activation of adjacent afferent and efferent axons of passage. Nicotine's spatial selectivity is exemplified by failure to elicit any response when it is injected in nearby fatty tissue sites or in the systemic circulation (Huang et al., 1993; Yuan et al., 1993).

Multi-electrode mapping of repolarization changes in unipolar recordings from single beats provides high-resolution estimates of the regional distribution of neurally-induced cardiac effects while avoiding the inconsistencies caused by physiological variations of neural responses in time (Pagé et al., 1995, 2006; Lall et al., 2008). Changes in the area of the unipolar waveform in response to a regional physiological intervention correlate with refractory period changes measured by the extrastimulus technique (Abildskov et al., 1980). In the ventricles, the repolarization wave (*T* wave) is well separated from the activation complex (RS) thereby providing an additional index in the form of activation-recovery intervals, which directly approximates refractory period changes in response to adrenergic stimulation (Millar et al., 1985).

Using such experimental approaches, we investigated the hypothesis that, beyond the right atrial and inferior vena cava-inferior left atrial ganglionated plexuses' predominant influences on the sinus and AV nodes, spatially divergent influences on atrial and ventricular indices are elicited by intrinsic cardiac neurons existing in all seven ganglionated plexuses.

2. Methods

This investigation conformed to Canadian Council for Animal Care and American Physiological Society's guidelines for the care and use of laboratory animals (World Medical Association, American Physiological Society, 2002) and was approved by an institutional animal care committee.

2.1. Animal preparation

Twenty two adult mongrel canines (either sex, 16–31 kg), were anaesthetized with thiopental (25 mg/kg iv, supplemented as required), intubated and ventilated. After thoracotomy exposing the heart, anaesthetic was changed to α-chloralose (50 mg/kg iv supplemented as required). A lead II ECG and blood pressure were recorded continuously. To investigate ventricular repolarization at fixed rate and to facilitate separation of atrial from ventricular unipolar wave forms during analysis, complete atrioventricular block was induced at the beginning of the experiment in 11 animals by formaldehyde (37%, 0.1–0.2 ml) injected into the AV node; thereafter, the ventricles were paced at 80/min via bipolar electrodes sutured onto the RV epicardium. AV block was induced midway during the experiment (before repeat nicotinic stimulation) in 6 experiments. Five preparations were studied with intact AV node.

2.2. Atrial and ventricular epicardial mapping

Multiple silicone plaques (carrying 127–191 unipolar recording contacts with 4.6–5.9 mm spacing) were positioned on the ventral, lateral and dorsal surfaces of the right and left atria (Pagé et al., 1995, 2006). A sock electrode array carrying 127 unipolar recording contacts (5–10 mm spacing) was positioned over the entire biventricular surface (Derakhchan et al., 1998). Unipolar leads were connected to a 256-channel recorder (EDI 12/256, École Polytechnique and Université de Montréal) controlled by PC-computer and custom-made software (Cardiomap III: www.crhsc.umontreal.ca/cardiomap). Unipolar recordings (with reference to limb leads) were amplified by programmable-gain analog amplifiers (0.05–450 Hz), converted to digital format at 1000 samples/s/channel and stored on hard disk from which files were retrieved for analysis. To assess the spatial distribution of neural effects at each atrial and ventricular site, the net area (integral) subtended by the unipolar electrogram was determined in recordings made prior to (basal) and at peak responses to nicotine (Pagé et al., 1995, 2006). In addition, ventricular repolarization intervals were determined by measuring the activation-recovery intervals from the maximum slope of negative deflections in activation complexes ($-dV/dt_{max}$) to maximum positive slope of *T* wave in each ventricular unipolar electrogram (Millar et al., 1985; Derakhchan et al., 1998). By algebraic subtraction of the integral value (or activation-recovery interval) of the basal beat from the corresponding value measured during ganglionic stimulation, difference maps are plotted indicating the atrial and ventricular regions that were affected by neural stimulation (Savard et al., 1991; Pagé et al., 2006).

2.3. Nicotinic stimulation of intrinsic cardiac ganglionated plexuses

As previously reported (Huang et al., 1993; Yuan et al, 1993), nicotine (usually 100 μg in 0.1 ml saline) was directly injected into loci within fatty tissues hosting each of the previously described 4 major atrial and 3 ventricular ganglionated plexuses (Fig. 1). Injections were limited to 1–3 loci *per* ganglionated plexus, depending on its size, thus minimizing the total amount of a chemical applied and avoiding leakage into the systemic circulation. Intervals of several minutes elapsed between injections to ensure recovery to base line values and to avoid tachyphylaxis (Blomquist and Priola, 1992).

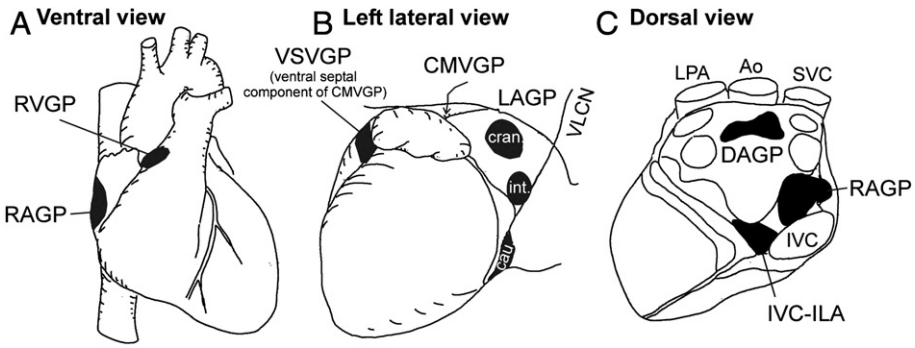

Fig. 1. Anatomical locations of the intrinsic cardiac ganglionated plexuses in the canine heart. A: ventral, B: left lateral, C: dorsal views of the heart. RAGP = right atrial ganglionated plexus (GP), RVGP = right ventricular GP, CMVGP = cranial medial ventricular GP, VSVGP = ventral septal ventricular GP, LAGP = left atrial GP, DAGP = dorsal atrial GP, IVC-ILA = inferior vena cava-inferior left atrial GP. VLCN = ventrolateral cardiac nerve, LPA = left pulmonary artery, Ao = aorta, IVC, SVC = inferior, superior vena cava.

Table 1
Incidences of changes in atrial rate elicited by nicotine injection into fatty tissues hosting individual ganglionated plexuses

	All changes	Bradycardia followed by tachycardia	Bradycardia alone	Tachycardia alone
RAGP	21/22	13/22	8/22	13/22
IVC-ILA	9/16	3/16	4/16	4/16
DAGP	8/10	2/10	3/10	6/10
LAGP	9/18	3/18	5/18	4/18
CMVGP	14/17	7/17	7/17	9/17
VSVGP	5/7	0/7	2/7	3/7
RVGP	6/11	2/11	2/11	4/11

Upper digits indicate the number of animals in which a given change in rhythm was identified in response to nicotine. When a change occurred in an individual preparation, a score of 1 is added without consideration for the number of injections. Lower digits indicate the number of animals in which a given ganglionated plexus was tested. Nicotine (100mcg in 0.1 ml) was injected into fatty tissues hosting either the right atrial (RA), the inferior vena cava-inferior left atrial (IVC-ILA), the dorsal atrial (DA), the left atrial (LA), the cranial medial ventricular (CMV), the ventral septal ventricular (VSV) or the right ventricular (RV) ganglionated plexus (GP).

2.4. Data analysis

A classical design of 2× 2 χ^2 analysis, *i.e.* 2 (right atrial or inferior vena cava-inferior left atrial ganglionated plexus *versus* all other ganglionated plexuses)×2 (effect/no effect) was used to test the hypotheses that 1) the incidence of atrial rate change in response to right atrial ganglionated plexus stimulation was significantly different from all other ganglionated plexuses combined, and 2) the incidence of AV conduction changes in response to inferior vena cava-inferior left atrial ganglionated plexus stimulation was significantly different from all other ganglionated plexuses combined. The atrial cycle length and other continuous variables (presented as mean±SD) were compared between basal state ("sinus rhythm") and at peak response using Student's *t*-test for paired data. Since the neurally-evoked cycle length changes were classified as either bradycardias or tachycardias, one-tailed *t*-test was employed to test the null hypothesis that the magnitude of the changes was not different from nought. The level of certainty for rejecting the null hypothesis was $p<0.05$. Differences in the magnitude of cycle length modification between the seven ganglionated plexuses were tested by univariate analysis of variance. Maps of regional atrial and ventricular repolarization changes in response to ganglionated plexus neuronal stimulation are presented as 1) selected examples in individual experiments or 2) cumulative maps indicating, for each recording site, the number of animals in which responses to a given ganglionated plexus were elicited beyond a threshold of +50 mV·ms (2×SD of changes in repeat measurements under basal conditions). Repolarization and AV conduction changes were measured at constant rate (atrial/ventricular pacing).

3. Results

The right atrial ganglionated plexus, which is embedded in a relatively large fat pad on the ventral aspect of the heart, was tested in all 22 animals (Table 1). The dorsal and ventral left atrial ganglionated plexuses were tested in fewer animals (Table 1: IVC-ILA in 16 animals, DAGP in 10, LAGP in 18). The cranial medial ventricular ganglionated plexus, a major ventricular ganglionated plexus, was tested in 17 animals but the smaller ventral septal and right ventricular ganglionated plexuses were identified and tested in 7 and in 11 animals, respectively.

3.1. Chronotropic and dromotropic responses

In 21 of 22 animals, loci were identified in the fatty tissues hosting the right atrial ganglionated plexus, at which nicotine injection elicited changes in atrial rate while remaining in "sinus" rhythm (Table 1: all changes). Specifically, the atrial rate changes were of the following 3 types: i) a biphasic response consisting of atrial cycle length prolongation (bradycardia) followed by cycle length shortening (tachycardia) as illustrated in the tachogram shown in Fig. 2A (identified in 13 animals), ii) bradycardia alone (13 animals), and iii) tachycardia alone (8 animals). The bradycardia responses occurred abruptly within ~20 s after nicotine injection whereas the tachycardia responses developed later reaching a maximum at ~90 s post-injection (Fig. 2A), in agreement with previous studies in which we also reported that the immediate bradycardias and slowly-developing tachycardias so elicited can be eliminated, respectively, by atropine and by β-adrenoceptor antagonists (Yuan et al., 1993; Yin et al., 1999). Atrial rate changes of several types were identified when nicotine injection was repeated at different loci in fatty tissues hosting the

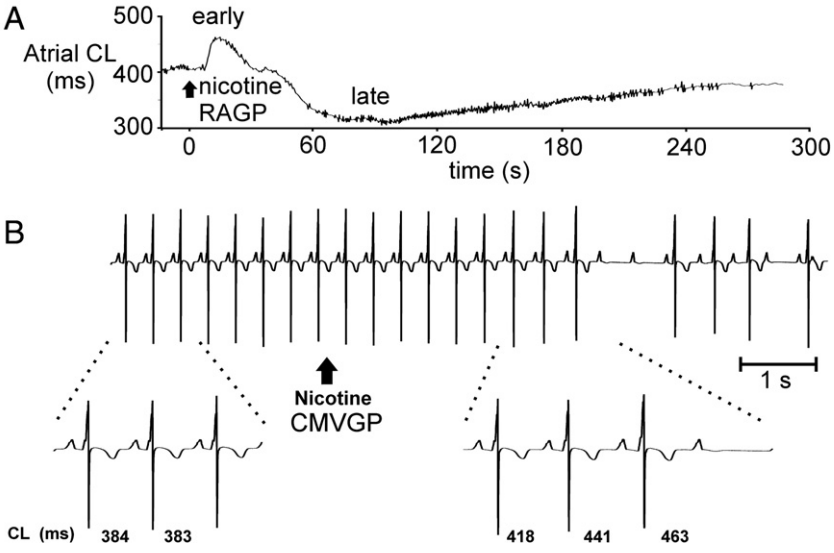

Fig. 2. Chronotropic and dromotropic effects in response to nicotinic stimulation of atrial and ventricular ganglionated plexuses. A. Computer-generated trace showing beat to beat variations in atrial cycle length following nicotine injection (0.1 ml; 100 μg) into the right atrial ganglionated plexus (RAGP) in the form of a typical biphasic response consisting of an abrupt bradycardia developing within ~20 s and a more slowly developing tachycardia peaking at ~90 s after injection. B. Surface lead ECG showing the negative chronotropic and dromotropic response to nicotine injection into a locus of the cranial medial ventricular ganglionated plexus (CMVGP): increase in sinus cycle length (CL, from 384 to 463 ms) followed by complete atrio-ventricular block.

right atrial ganglionated plexus in individual preparations (explaining why, in Table 1, the summed numbers of atrial rate changes of the 3 types exceed the numbers of animals tested).

Bradycardias and tachycardias were elicited by nicotinic stimulation of neurons in all other ganglionated plexuses (Table 1 and Fig. 3A), albeit less consistently than in response to right atrial ganglionated plexus neurons ($p=0.005$ by χ^2 analysis). The incidences of the chronotropic responses observed among the tested preparations ranged from 50–60% (Fig. 3A: IVC-ILA, LAGP, RVGP) to 70–80% (DAGP, CMVGP, VSVGP). Statistically significant changes in atrial cycle length were identified during the bradycardias (Table 2A) and the tachycardias (Table 2B) evoked by nicotinic stimulation of 6 of the 7 ganglionated plexuses, excepting the ventral septal ventricular ganglionated plexus. However, no statistically significant difference in the magnitudes of the responses was identified between the ganglionated plexuses. Nonetheless, the most pronounced bradycardias were induced in response to stimulation of neurons of the right atrial, the cranial medial and the right ventricular ganglionated plexuses.

Table 2
Changes in atrial cycle length (ms) elicited by nicotine injection into fatty tissues hosting individual ganglionated plexuses

	A. Bradycardia				B. Tachycardia			
	n	Basal	Nicotine	Δ%	*n*	Basal	Nicotine	Δ%
RAGP	33	407±64	514±298	+28±81*	27	416±62	382±57	−8±6*
IVC-ILA	6	385±89	440±78	+16±14*	8	381±60	349±54	−8±8*
DAGP	7	370±27	419±50	+13±9*	5	409±79	366±64	−10±7*
LAGP	7	376±42	457±103	+22±30*	14	377±39	342±49	−9±8*
CMVGP	12	374±43	511±260	+33±52*	16	432±79	356±61	−16±14*
VSVGP	3	374±26	397±24	+6±4	2	420±30	390±5	−7±6
RVGP	7	387±60	544±257*	+36±49*	6	412±38	372±24	−9±7*

Data are mean±SD; *n*=number of responses; *$p<0.05$ by paired *t*-test (one-tailed). Nicotine (100mcg in 0.1 ml) was injected into fatty tissues hosting either the right atrial (RA), the inferior vena cava-inferior left atrial (IVC-ILA), the dorsal atrial (DA), the left atrial (LA), the cranial medial ventricular (CMV), the ventral septal ventricular (VSV) or the right ventricular (RV) ganglionated plexus (GP).

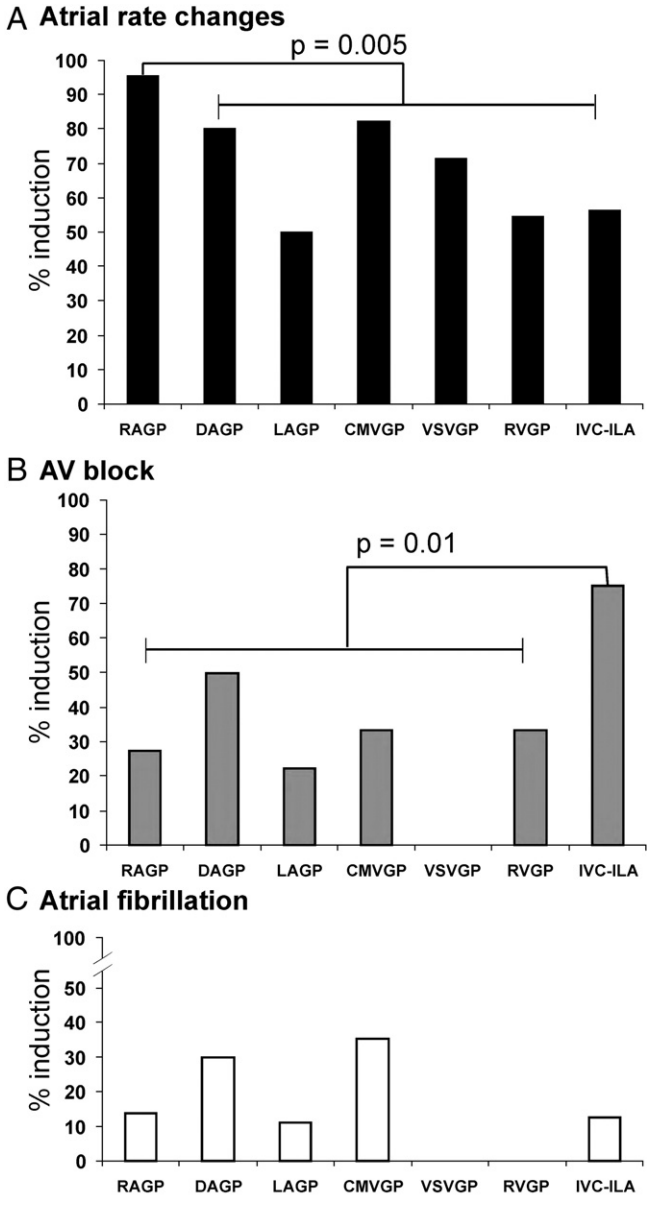

Fig. 3. Incidences of changes in atrial rate, AV conduction and tachyarrhythmia induction elicited by nicotine injection into individual ganglionated plexuses. Bar graphs show the proportion of animals (expressed as %) in which changes in atrial rate (A), AV block (B) or atrial fibrillation (C) were identified in response to nicotine injection into each of the seven ganglionated plexuses (same abbreviations as in Fig. 1). When a given change occurred in an individual preparation, a score of 1 is added in computing the proportion without considering the number of repeat trials *per* ganglionated plexus.

Prolongation of AV conduction or AV block was elicited in response to nicotinic stimulation of neurons in 6 of the 7 ganglionated plexuses, as illustrated in Fig. 2B (in which bradycardia was followed by AV block in response to CMVGP neuronal stimulation). However, such changes in AV conduction occurred most consistently following neuronal stimulation in the inferior vena cava-inferior left atrial ganglionated plexus (Fig. 3B: significantly different from the other ganglionated plexuses, $p=0.01$ by χ^2 analysis).

3.2. Atrial tachyarrhythmias

Atrial premature depolarizations followed by atrial tachyarrhythmias (fibrillation) were elicited in response to nicotinic stimulation of atrial ganglionated plexus neurons in a minority of preparations (Fig. 3C). Such responses occurred most frequently after stimulation of cranial medial ventricular ganglionated plexus neurons.

3.3. Atrial unipolar wave form changes

Changes in the atrial repolarization wave form at each of the multielectrode recording sites (Fig. 4A) were assessed as the difference between the area (integral) subtended by the unipolar electrogram at peak effect after nicotine injection minus its area in basal beats as illustrated in Fig. 4B. Representative recordings show marked positive changes following nicotine injection (site 1), slight positive changes (site 2) and reciprocal (negative) changes (site 3). Marked positive changes were consistently identified regionally in the right atrial free wall within ~20 s after nicotine injection into fatty tissues hosting the right atrial ganglionated plexus (Fig. 4C). Such regional changes were identified concomitantly with chronotropic responses to neuronal stimulation as well as when atrial rate was fixed by pacing (Pagé et al., 1995, 2006).

Interestingly, regional atrial changes were also elicited in response to nicotine injection into fatty tissues hosting ventricular ganglionated plexuses. Fig. 4D shows that unipolar wave form changes were identified in the right atrial free wall in response to nicotinic stimulation of right ventricular ganglionated plexus neurons, occurring with a similar distribution as in response to stimulation of right atrial ganglionated plexus neurons in the same preparation (Fig. 4C).

3.4. Ventricular unipolar wave form changes

Changes in the ventricular repolarization wave form were identified at ~90 s following nicotine injection into fatty tissues hosting the right atrial ganglionated plexus. In the trial illustrated in Fig. 5,

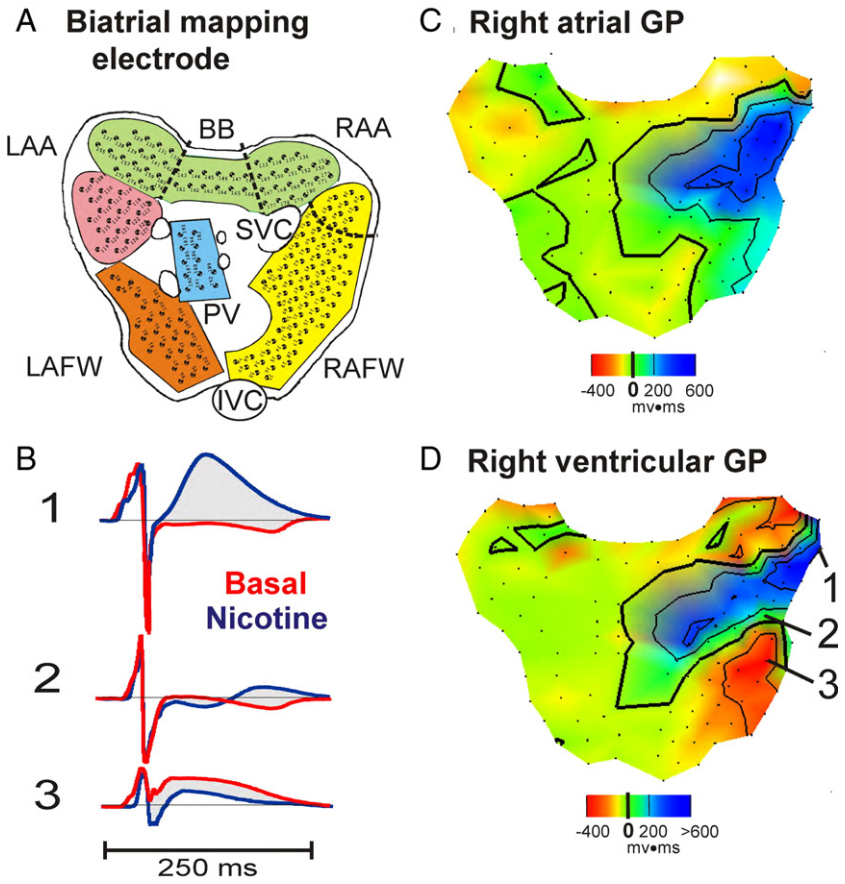

Fig. 4. Atrial unipolar wave form changes induced in response to nicotinic stimulation of either an atrial or a ventricular ganglionated plexus. A. Epicardial plaque-electrodes positioned on 1) Bachmann's bundle (BB, green), 2) the right atrial free wall (RAFW) and lateral right atrial appendage (RAA, yellow), 3) the inferior dorsal left atrial free wall (LAFW, orange), 4) the lateral left atrial appendage (LAA, pink), 5) the dorsal LA wall between the pulmonary veins (blue). B. Representative unipolar recordings under basal conditions (red tracing) and after nicotine injection into fatty tissues hosting the ganglionated plexuses (blue tracing). Changes in the atrial repolarization wave form at each site are assessed as the difference between the electrogram area at peak nicotine effect minus basal. C,D. Changes are represented as color codes ranging from diffuse slightly negative (yellow, orange) to markedly positive changes (blue) in the right atrial wall. Note that marked changes were induced in the right atrium in response to nicotine injection into either the right atrial (C: RAGP) or right ventricular ganglionated plexus (D: RVGP). Such regional changes occurred concomitantly with the early phase (bradycardia) of the biphasic atrial chronotropic responses. (For interpretation of the references to colour in this figure legend, the reader is referred to the web version of this article.)

increases in *T* wave amplitude or changes in wave form polarity from negative to positive *T* waves were identified throughout the posterior right ventricular wall and left ventricular apical regions (panel A) as illustrated with electrograms "a" (slight change: light grey areas) and "b" (marked changes: grey or dark areas). Concomitantly, activation-recovery intervals shortened (panel B) in the areas in which marked unipolar wave form changes were identified. Such changes were reproducible with repeat nicotine injection at the same locus (not shown). Reciprocal changes consisting of *T* wave amplitude reduction and repolarization interval prolongation were identified at a few sites in the lateral right ventricular wall (panel A: hatched).

3.5. Cumulative maps

Data derived from several experiments are summarized in the form of cumulative maps (Fig. 6) in which the number plotted at each recording site indicates the number of animals that displayed significant unipolar wave form changes in response to nicotinic stimulation of intrinsic cardiac neurons existing within each of the two major—atrial and ventricular—ganglionated plexuses.

In response to nicotine injection into fatty tissues hosting the right atrial ganglionated plexus, atrial changes were identified in the right atrial free wall in the sinus node region (Fig. 6A: left hand map) as illustrated above in an individual preparation (Fig. 4C). Ventricular changes elicited by nicotinic stimulation of right atrial ganglionated plexus neurons were identified in various regions in different preparations, but most frequently in the posterior right ventricular wall (Fig. 6A: right hand map, green color-coded region) as illustrated above in an individual preparation (Fig. 5). Such changes were identified at constant ventricular rate (formaldehyde-induced AV block and ventricular pacing) and occurred concomitantly with the positive chronotropic atrial responses (*i.e.* ~90 s after nicotine injection).

In response to nicotine injection into fatty tissues hosting the cranial medial ventricular ganglionated plexus, regional changes were identified in both the right and left atria (Fig. 6B: left hand maps). Ventricular changes in the same 12 preparations were identified extensively throughout the ventricular surfaces (Fig. 6B—right hand maps: extensive green and blue color-coded regions). It is also noteworthy that the ventricular changes occurred with higher incidences in response to cranial medial ventricular (Fig. 6B—right hand) than in response to right atrial (Fig. 6A—right hand) ganglionated plexus stimulation. Ventricular changes in response to nicotinic stimulation of cranial medial ventricular ganglionated plexus neurons were identified at a constant ventricular rate and occurred concomitantly with the later (adrenergic) phase of the biphasic atrial chronotropic response (*i.e.* ~90 s after nicotine injection).

4. Discussion

Novel findings reported herein are that i) intrinsic cardiac neurons from all 7 ganglionated plexuses may be involved in atrial chronotropic and AV nodal regulation, ii) the repolarization properties of ventricular

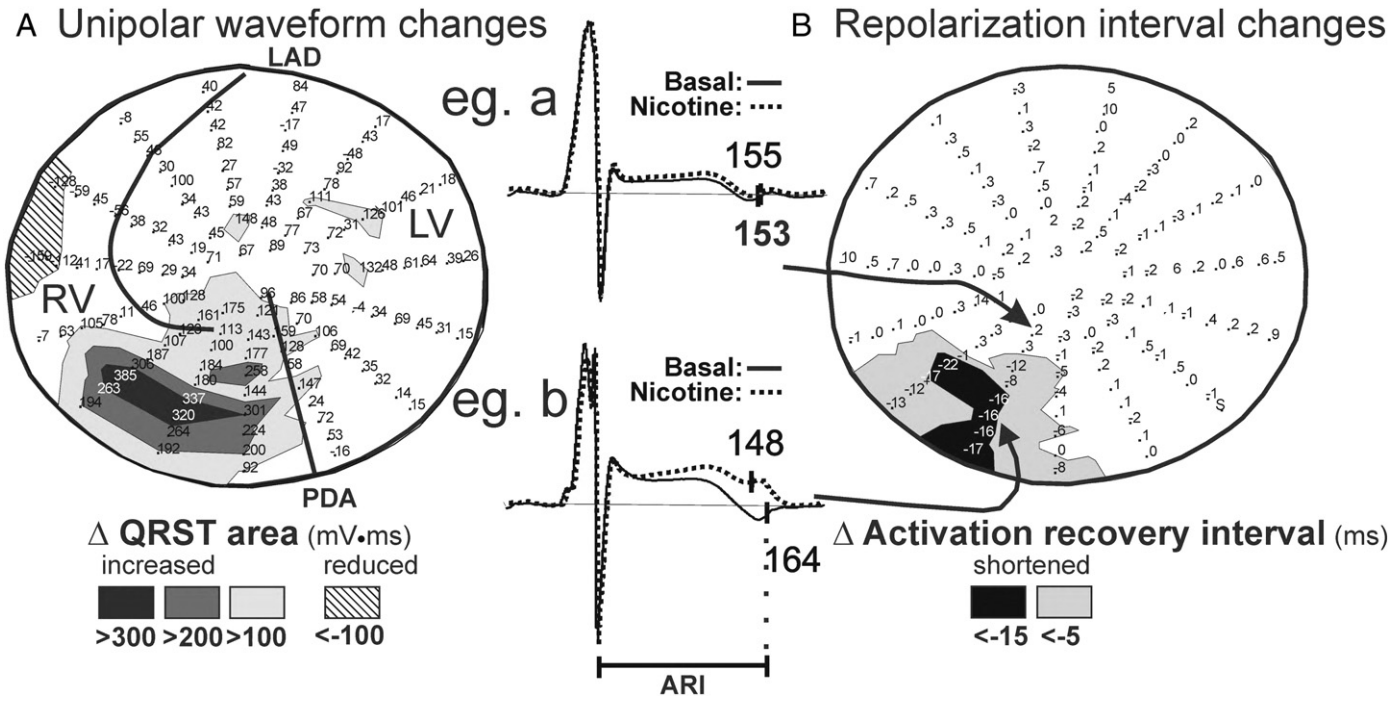

Fig. 5. Ventricular unipolar wave form changes in response to nicotinic stimulation of right atrial ganglionated plexus (RAGP) neurons. Regional changes in QRST area (A) or activation-recovery intervals (B) are depicted in response to nicotine injection into fatty tissues hosting the RAGP. In the polar representation, the base of the right and left ventricles (RV, LV) are along the circumference, and the LV apex at the center; the left anterior descending (LAD) and posterior descending (PDA) coronary arteries are indicated coursing from basal to apical regions. Ventricular repolarization changes were identified at 90 s after injection as regional increases in QRST area (A: light grey: >100 mV·ms, grey: >200 mV·ms, dark: >300 mV·ms) localized mainly to the posterior RV wall and LV apex. At most of these locations, shortening of the activation-recovery intervals were also identified (B: grey: −5 ms, dark: −15 ms or more). Reciprocal changes (hatched: slight QRST area reductions) were identified at a few RV lateral basal loci (A).

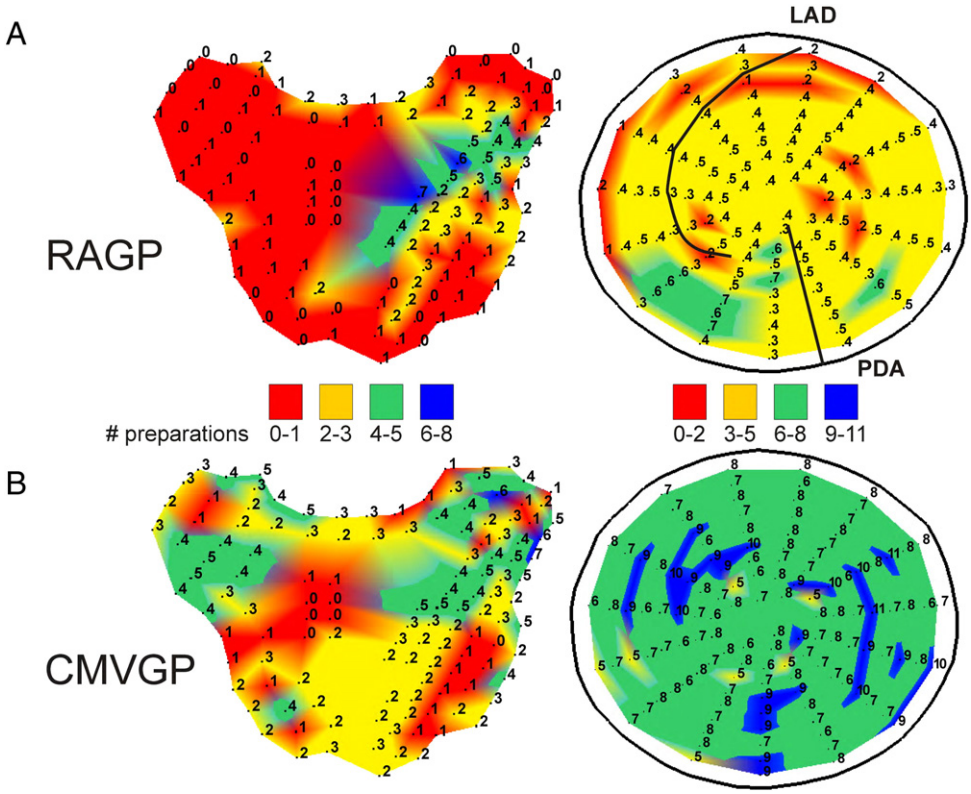

Fig. 6. Cumulative incidences of regional atrial and ventricular unipolar wave form changes in response to nicotinic stimulation of the right atrial (A: RAGP) and cranial medial ventricular ganglionated plexus (B: CMVGP) neurons. Color-coded maps show for each recording site the cumulative incidences, among animals (upper left: $n=10$, other panels: $n=12$ preparations), of the ones showing significant neurally-induced changes (>+50 mV·ms). Atrial changes in response to RAGP stimulation were identified in the RA wall whereas biatrial changes were elicited by CMVGP stimulation (left hand maps). Ventricular changes determined at fixed rate were identified most frequently in the posterior RV wall in response to RAGP stimulation but a more extensive spatial distribution and a higher incidence in response to CMVGP neuronal stimulation (right hand maps).

muscle can be influenced by atrial (*e.g.* right atrial) as well as by ventricular ganglionated plexus neurons (*e.g.* cranial medial ventricular), and iii) in spite of such spatially divergent influences, distinct regional patterns of unipolar wave form changes are identified in response to nicotinic stimulation of individual ganglionated plexuses.

4.1. Redundant regulation of chronotropic and dromotropic functions

The present study, performed employing nicotinic stimulation of ganglionated plexus neurons without affecting axons of passage, expands recent findings that electrical stimulation applied to left as well as to right atrial ganglionated plexuses influences sinus and AV nodal functions (Hou et al., 2007). While confirming the predominant role of the right atrial and the inferior vena cava-inferior left atrial ganglionated plexuses in chronotropic and dromotropic regulation, respectively, this study extends to intrinsic cardiac neurons existing in all 7 ganglionated plexuses some chronotropic and dromotropic regulatory capacity.

We have previously reported that acute decentralization (bilateral vagotomy and stellectomy) reduces the incidences of chronotropic and inotropic responses to nicotine injection into the right atrial and into the cranial medial ventricular ganglionated plexuses by ~33% and ~25%, respectively (Yuan et al., 1993), suggesting that central neurons might be involved in the generation of a subset of such responses. Moreover, neuronal interactions occurring within the intrinsic cardiac nervous system can contribute to the generation of chronotropic and dromotropic responses independently from the central nervous system (Hou et al., 2007; Randall et al., 2003).

4.2. Spatially divergent influences of atrial and ventricular ganglionated plexuses

The data reported herein support the notion that the canine ventricles are under the influence of postganglionic autonomic axons which arise from atrial as well as from ventricular ganglia (Blomquist et al., 1987). Neurally-mediated unipolar wave form changes followed distinctive spatial patterns, depending on the individual ganglionated plexus being stimulated. Ventricular repolarization changes elicited by right atrial ganglionated plexus stimulation were most frequently localized in the posterior right ventricular wall, with a lower incidence of effects in the anterior right and left ventricular wall and apex. In contrast, generalized ventricular repolarization changes were identified in response to nicotinic stimulation of cranial medial ventricular ganglionated plexus neurons. It is important to note that the changes were identified at constant ventricular rate (AV block and ventricular pacing). Such changes frequently occurred concomitantly with positive chronotropic atrial responses, suggesting that shortening of ventricular repolarization intervals might occur in response to activation of efferent adrenergic neurons located throughout the intrinsic cardiac nervous system.

We have previously reported that the positive inotropic effects assessed from 4 ventricular loci in response to nicotinic stimulation of cranial medial ventricular ganglionated plexus neurons are not abolished following decentralization (Yuan et al., 1993). The most straightforward interpretation of such neuronal influences on regional ventricular repolarization properties is that they result from activation of efferent autonomic neurons projecting to the ventricles (Dickerson et al., 1998).

Nicotinic stimulation of right atrial and right ventricular ganglionated plexus neurons elicited changes restricted to the right atrial wall whereas both right and left atrial changes were elicited in response to stimulation of cranial medial ventricular ganglionated plexus neurons. The data therefore suggest that atrial electrical events can be modulated via neuronal interactions in which are involved nicotine sensitive neurons existing within ventricular ganglionated plexuses.

That neurons in each major ganglionated plexus have the capacity of influencing widely dispersed cardiac regions is not surprising given recent anatomical (Gray et al, 2004) and functional data (Randall et al., 2003; Waldmann et al., 2006) indicating that neurons in different intrinsic cardiac ganglionated plexuses are in constant communication with one another.

4.2.1. Limitations

Influences on atrial and ventricular indices were demonstrated in a variable proportion of animals for each ganglionated plexus. This does not necessarily imply that an animal in which a response failed to be elicited did not have the capacity to generate one, since the effective neuronal population may have been missed depending of the injection site. Indeed, responses failed to be elicited by nicotine injection at some loci in the fat pad hosting a ganglionated plexus even when responses were evoked from other injection sites. Moreover, to minimize the amount of drug applied and to avoid tachyphylaxis, the number of nicotine injections was limited to 1–3 loci *per* fat pad hosting a given ganglionated plexus, depending on its size. However, similar responses were obtained whenever nicotine injection was repeated at an active locus. Failure to elicit a detectable response from a given injection site presumably was due to the absence of neurons in its vicinity, to the local neuronal population's lack of sensitivity to nicotine, or to nicotine administration in quantities insufficient to activate a sufficient population of neurons to engender detectable responses. There was also variability in the responses to nicotine when injected at different loci in fat hosting a given ganglionated plexus. For instance, bradycardia alone, sinus tachycardia alone, or biphasic chronotropic responses were elicited from different loci in the fat pad hosting the right atrial ganglionated plexus. Such variability of the responses to nicotinic stimulation is consistent with the varied functional and differential neuroanatomy characteristics of this nervous system.

Small amounts of formaldehyde were injected for AV node ablation, thus minimizing the risk of neuronal damage. Moreover, similar responses were recorded with intact AV node or following its chemical ablation when responses occurred at comparable rates.

Among the arguments linking the physiological responses to local modulation of intrinsic cardiac neuronal activity, one should consider that 1) systemic administration of nicotine at the doses employed for local injection did not elicit any response and 2) biphasic chronotropic responses similar to the ones identified herein can be elicited by nicotine when administered into the sinus node artery in either isolated right atrial preparations perfused *in vitro* (Yin et al., 1999) or in intact preparations (Yuan et al., 1993). The immediate bradycardias and slowly-developing tachycardias so elicited can be eliminated by atropine and β-adrenoceptor antagonists, respectively (Yuan et al., 1993; Yin et al., 1999). Further experiments are required to address the dependence of the ventricular influences reported herein on muscarinic cholinergic *versus* adrenergic myocardial receptor activation.

In contrast to the redundant control of sinus and AV nodal functions reported herein, it has been reported that the right atrial and inferior vena cava-inferior left atrial ganglionated plexus equivalents in humans display greater selectivity for one or the other when subjected to electrical stimulation (Quan et al., 1999, 2002). This could represent a species difference between humans and canines but it might also indicate that intraoperative conditions and electrical stimulation protocols employed in humans failed to elicit neuronal interactions that might occur with greater consistency in response to local pharmacological stimulation of somata and dendrites within intrinsic cardiac ganglionated plexuses.

4.2.2. Perspectives

Data derived from this study indicate that spatially divergent and overlapping cardiac regions are under the influence of neurons distributed throughout the intrinsic cardiac nervous system. Intrinsic cardiac neurons, when excessively activated, can initiate ventricular

(Huang et al., 1994) and atrial (Armour et al., 2005) tachyarrhythmias as well as exacerbate ventricular ischemia (Cardinal et al., 2004). In fact, ganglionated plexus ablation is currently under investigation as an adjunct to catheter-based or surgical therapies of atrial tachyarrhythmias (Davis and Jacobs, 2003, Alex and Guvendik, 2005, Lemery et al., 2006, Mehall et al., 2007, White et al., 2007, Pokushalov, 2008). That they exert redundant control over diverse cardiac regions suggests that it may be possible to target these neurons for ablation and attenuate their influence without completely suppressing autonomic regulation. However as a corollary, ablating or activating an anatomically discrete population of neurons will not necessarily produce selective and controlled modification of a given cardiac index. Moreover, redundancy of control may be involved in recovery of function following epicardial fat pad ablation (Oh et al., 2006) or in limiting the effects of neuropathology. Data derived from this study indicate that when contemplating targeting neurons involved in arrhythmia formation, neurons located in multiple ganglionated plexuses will have to be considered.

Acknowledgements

The authors gratefully acknowledge the technical assistance of Ms. Caroline Bouchard. This study was supported by the Canadian Institutes of Health Research, the Heart & Stroke Foundation of Quebec, and the National Institutes of Health.

References

Abildskov, J.A., Evans, A.K., Lux, R.L., Burgess, M.J., 1980. Ventricular recovery properties and QRST deflection area in cardiac electrograms. Am. J. Physiol, Heart Circ. Physiol. 239, H227–H231.

Alex, J., Guvendik, L., 2005. Evaluation of ventral cardiac denervation as a prophylaxis against atrial fibrillation after coronary artery bypass grafting. Ann. Thorac. Surg. 79, 517–520.

Ardell, J.L., Randall, W.C., 1986. Selective vagal innervation of sinoatrial and atrioventricular nodes in canine heart. Am. J. Physiol, Heart Circ. Physiol. 251, H764–H773.

Armour, J.A., 2004. Cardiac neuronal hierarchy in health and disease. Am. J. Physiol. Integr. Comp. Physiol. 287, R262–R271.

Armour, J.A., Murphy, D.A., Yuan, B.X., MacDonald, S., Hopkins, D.A., 1997. Gross and microscopic anatomy of the human intrinsic cardiac nervous system. Anat. Rec. 247, 289–298.

Armour, J.A., Richer, L.P., Pagé, P., Vinet, A., Kus, T., Vermeulen, M., Nadeau, R., Cardinal, R., 2005. Origin and pharmacological response of atrial tachyarrhythmias induced by discrete activation of mediastinal nerves in canines. Auton. Neurosci.: Basic Clin. 118, 68–78.

Blomquist, T.M., Priola, D.V., 1992. Tachyphylaxis of the intrinsic cardiac nerves to nicotine: effects on A-V nodal conduction. J. Auton. Pharmacol. 12, 51–59.

Blomquist, T.M., Priola, D.V., Romero, A.M., 1987. Source of intrinsic innervation of canine ventricles: a functional study. Am. J. Physiol, Heart Circ. Physiol. 252, H638–H644.

Bojsen-Moller, F., Tranum-Jensen, J., 1971. Whole-mount demonstration of cholinesterase-containing nerves in the right atrial wall, nodal tissue, and atrioventricular bundle. J. Anat. 108, 375–386.

Butler, C.K., Smith, F.M., Nicholson, J., Armour, J.A., 1990a. Cardiac effects induced by chemically activated neurons in canine intrathoracic ganglia. Am. J. Physiol, Heart Circ. Physiol. 259, H1108–H1117.

Butler, C.K., Smith, F.M., Cardinal, R., Murphy, D.A., Hopkins, D.A., Armour, J.A., 1990b. Cardiac responses to electrical stimulation of discrete loci in canine atrial or ventricular ganglionated plexi. Am. J. Physiol, Heart Circ. Physiol. 259, H1365–H1373.

Cardinal, R., Ardell, J.L., Linderoth, B., Vermeulen, M., Foreman, R.D., Armour, J.A., 2004. Spinal cord stimulation differentially modulates ischaemic electrical responses to different stressors in canine ventricles. Auton. Neurosci.: Basic Clin. 111, 37–47.

Chiou, C.W., Eble, J.N., Zipes, D.P., 1997. Efferent vagal innervation of the canine atrial and sinus and atrioventricular nodes. The third fat pad. Circulation 95, 2573–2584.

Davis, Z., Jacobs, H.K., 2003. Aortic fat pad destruction and post operative atrial fibrillation. Card. Electrophysiol. Rev. 7, 185–188.

Derakhchan, K., Cardinal, R., Brunet, S., Klug, D., Pharand, C., Kus, T., Sasyniuk, B.I., 1998. Polymorphic ventricular tachycardias induced by D-sotalol and phenylephrine in canine preparations of atrioventricular block: initiation in the conduction system followed by spatially unstable re-entry. Cardiovasc. Res. 38, 617–630.

Dickerson, L.W., Rodak, D.J., Fleming, T.J., Gatti, P.J., Massari, V.J., McKenzie, J.C., Gillis, R.A., 1998. Parasympathetic neurons in the cranial medial ventricular fat pad on the dog heart selectively decrease ventricular contractility. J. Auton. Nerv. Syst. 70, 129–141.

Gatti, P.J., Johnson, T.A., Phan, P., Jordan, I.K., Coleman, W., Massari, V.J., 1995. The physiological and anatomical demonstration of functionally selective parasympathetic ganglia located in discrete fat pads on the feline heart. J. Auton. Nerv. Syst. 51, 255–259.

Gray, A.L., Johnson, T.A., Ardell, J.L., Massari, V.J., 2004. Parasympathetic control of the heart. II. A novel interganglionic intrinsic cardiac circuit mediates neural control of heart rate. J. Appl. Physiol. 96, 2273–2278.

Hou, Y., Scherlag, B.J., Lin, J., Zhou, J., Song, J., Zhang, Y., Patterson, E., Lazzara, R., Jackman, W.M., Po, S.S., 2007. Interactive atrial neural network: determining the connections between ganglionated plexi. Heart Rhythm 4, 56–63.

Huang, M.H., Smith, F.M., Armour, J.A., 1993. Modulation of in situ canine intrinsic cardiac neuronal activity by nicotine, muscarinic, and β-adrenergic agonists. Am. J. Physiol., Regul. Integr. Comp. Physiol. 265, R659–R669.

Huang, M.H., Wolf, S.G., Armour, J.A., 1994. Ventricular arrhythmias induced by chemically modified intrinsic cardiac neurons. Cardiovasc. Res. 28, 636–642.

Lall, S.C., Foyil, K.V., Sakamoto, S., Voeller, R.K., Boineau, J.P., Damiano Jr., R.J., Schuessler, R.B., 2008. Pulmonary vein isolation and the Cox maze procedure only partially denervate the atrium. J. Thorac. Cardiovasc. Surg. 135, 894–900.

Lazzara, R., Scherlag, B.J., Robinson, M.J., Samet, P., 1973. Selective in situ parasympathetic control of the canine sinoatrial and atrioventricular nodes. Circ. Res. 32, 393–410.

Lemery, R., Birnie, D., Tang, A.S.L., Green, M., Gollob, M., 2006. Feasibility study of endocardial mapping of ganglionated plexuses during catheter ablation of atrial fibrillation. Heart Rhythm 3, 387–396.

Mehall, J.R., Kohut, R.M., Schneeberger, E.W., Taketani, T., Merrill, W.H., Wolf, R.K., 2007. Intraoperative epicardial electrophysiologic mapping and isolation of autonomic ganglionated plexi. Ann. Thorac. Surg. 83, 538–541.

Millar, C.K., Kralios, F.A., Lux, R.L., 1985. Correlation between refractory periods and activation-recovery intervals from elecrograms: effects of rate and adrenergic interventions. Circulation 72, 1372–1379.

Oh, S., Zhang, Y., Bibevski, S., Marrouche, N.F., Natale, A., Mazgalev, T.N., 2006. Vagal denervation and atrial fibrillation inducibility: epicardial fat pad ablation does not have long-term effects. Heart Rhythm 3, 701–708.

Pagé, P., Dandan, N., Savard, P., Nadeau, R., Armour, J.A., Cardinal, R., 1995. Regional distribution of atrial electrical changes induced by stimulation of extracardiac and intracardiac neural elements. J. Thorac. Cardiovasc. Surg. 109, 377–388.

Pagé, P., Armour, J.A., Yin, Y., Vermeulen, M., Nadeau, R., Cardinal, R., 2006. Differential effects of cervical vagosympathetic and mediastinal nerve activation on atrial arrhythmia formation in dogs. Auton. Neurosci.: Basic Clin. 128, 9–18.

Pauza, D.H., Skripka, V., Pauziene, N., Stropus, R., 1999. Anatomical study of the neural ganglionated plexus in the canine right atrium: implications for selective denervation and electrophysiology of the sinoatrial node in dog. Anat. Rec. 255, 271–294.

Pauza, D.H., Skripka, V., Pauziene, N., Stropus, R., 2000. Morphology, distribution, and variability of the epicardiac neural ganglionated subplexuses in the human heart. Anat. Rec. 259, 353–382.

Pauza, D.H., Skripka, V., Pauziene, N., 2002. Morphology of the intrinsic cardiac nervous system in the dog: a whole-mount study employing histochemical staining with acetylcholinesterase. Cells Tissues Organs 172, 297–320.

Pokushalov, E., 2008. The role of autonomic denervation during catheter ablation of atrial fibrillation. Curr. Opin. Cardiol. 23, 55–59.

Priola, D.V., Spurgeon, H.A., Geis, W.P., 1977. The intrinsic innervation of the canine heart: a functional study. Circ. Res. 40, 50–56.

Quan, K.J., Lee, J.H., Geha, A.S., Biblo, L.A., Van Hare, G.F., Mackall, J.A., Carlson, M.D., 1999. Characterization of sinoatrial parasympathetic innervation in humans. J. Cardiovasc. Electrophysiol. 10, 1060–1065.

Quan, K.J., Lee, J.H., Van Hare, G.F., Biblo, L.A., Mackall, J.A., Carlson, M.D., 2002. Identification and characterization of atrioventricular parasympathetic innervation in humans. J. Cardiovasc. Electrophysiol. 13, 735–739.

Randall, D.C., Brown, D.R., McGuirt, A.S., Thompson, G.W., Armour, J.A., Ardell, J.L., 2003. Interactions within the intrinsic cardiac nervous system contribute to chronotropic regulation. Am. J. Physiol., Regul. Integr. Comp. Physiol. 285, R1066–R1075.

Savard, P., Cardinal, R., Nadeau, R.A., Armour, J.A., 1991. Epicardial distribution of ST segment and T wave changes by stimulation of intrathoracic ganglia and cardiopulmonjary nerves in dogs. J. Auton. Nerv. Syst. 34, 47–58.

Smith, F.M., 1999. Extrinsic inputs to intrinsic neurons in the porcine heart in vitro. Am J. Physiol., Regul. Integr. Comp. Physiol. 276, R455–R467.

Takahashi, N., Barber, M.J., Zipes, D.P., 1985. Efferent vagal innervation of canine ventricle. Am. J. Physiol, Heart Circ. Physiol. 248, H89–H97.

Tsuboi, M., Furukawa, Y., Nakajima, K., Kurogouchi, F., Chiba, S., 2000. Inotropic, chronotropic, and dromotropic effects mediated via parasympathetic ganglia in the dog heart. Am. J. Physiol, Heart Circ. Physiol. 279, H1201–H1207.

Waldmann, M., Thompson, G.W., Kember, G.C., Ardell, J.L., Armour, J.A., 2006. Stochastic behavior of atrial and ventricular intrinsic cardiac neurons. J. Appl. Physiol. 101, 413–419.

White, C.M., Sander, S., Coleman, C.I., Gallagher, R., Takata, H., Humphrey, C., Henyan, N., Gillespie, E.L., Kluger, J., 2007. Impact of epicardial anterior fat pad retention on postcardiothoracic surgery atrial fibrillation incidence. The AFIST-III Study. J. Am. Coll. Cardiol. 49, 298–303.

World Medical Association, American Physiological Society, 2002. Guiding principles for research involving animals and human beings. Am. J. Physiol., Regul. Integr. Comp. Physiol. 283, R281–R283.

Yin, Y.L., Pagé, P., Cardinal, R., 1999. Concentration-dependent effects of angiotensin II on sinus rate in canine isolated right atrial preparations. Can. J. Physiol. Pharmacol. 77, 36–41.

Yuan, B.X., Ardell, J.L., Hopkins, D.A., Armour, J.A., 1993. Differential cardiac responses induced by nicotinic sensitive canine atrial and ventricular neurons. Cardiovasc. Res. 27, 760–769.

Yuan, B.X., Ardell, J.L., Hopkins, D.A., Losier, A.M., Armour, J.A., 1994. Gross and microscopic anatomy of canine intrinsic cardiac neurons. Anat. Rec. 239, 75–87.